

A robust method for filling in masked data in astronomical images

PIETER VAN DOKKUM¹

¹*Astronomy Department, Yale University, 219 Prospect St, New Haven, CT 06511, USA*

Submitted to PASP

ABSTRACT

Astronomical images often have regions with missing or unwanted information, such as bad pixels, bad columns, cosmic rays, masked objects, or residuals from imperfect model subtractions. In certain situations it can be essential, or preferable, to fill in these regions. Most existing methods use low order interpolations for this task. In this paper a method is described that uses the full information that is contained in the pixels just outside masked regions. These edge pixels are extrapolated inwards, using iterative median filtering. This leads to a smoothly varying spatial resolution within the filled-in regions, and ensures seamless transitions between masked pixels and good pixels. Gaps in continuous, narrow features can be reconstructed with high fidelity, even if they are large. The method is implemented in `maskfill`, an open-source MIT licensed Python script.[†] Its performance is illustrated with several examples.

Keywords: Direct imaging (387) — Astronomical techniques (1684) — Astronomy data reduction (1861) — Astronomy data analysis (1858)

1. INTRODUCTION

Image masking serves various purposes. Detector defects, such as hot pixels, bad pixels, or bad columns, result in predictable locations where data cannot be trusted or are missing altogether. Cosmic ray hits can occur anywhere on the detector, producing short trails of very bright pixels (Leach & Gursky 1979). Both detector defects and cosmic rays are routinely masked in the early stages of the data reduction process.

Another reason for masking is if certain objects are unwanted. An example is masking of bright stars and galaxies in data that are searched for low surface brightness emission (Greco et al. 2018; Montes & Trujillo 2018; Danieli & van Dokkum 2019). A variation on this theme is the masking of residuals after image subtraction. Image subtraction is routinely performed in transient photometry (Kessler et al. 2015), searches for faint or spatially-extended objects near bright ones (Marois et al. 2006; van Dokkum et al. 2020), continuum correction of narrow band data (James et al. 2004; Garner et al. 2022; Lokhorst et al. 2022), and a wide range of

other contexts. In all these applications, regions where the subtraction is not satisfactory (such as the centers of bright stars) are typically masked, so they do not impact the subsequent analysis.

In many cases masked pixels do not need to be filled in, either because there are independent, redundant, observations of the same sky positions (e.g., Fruchter & Hook 2002), or because subsequent image analysis steps can explicitly handle masked data (such as the GALFIT profile fitting software; Peng et al. 2002).

However, there are exceptions. Multiple redundant exposures are not always available, for instance in time series data. Also, detector defects and cosmic rays are sharp features that are best identified before resampling the data; this is why reduction pipelines often remove these features from individual frames, even if multiple exposures are available (Kelson 2003; Neill et al. 2023). Turning to masked stars and galaxies, convolutions such as Gaussian smoothing produce artifacts on both sides of sharp boundaries, and these can be greatly reduced when the masks are (temporarily) filled in beforehand. Another reason to fill in masks is to properly account for missing flux when measuring intracluster light (Montes & Trujillo 2018), Galactic cirrus emission (Liu et al. 2023) or other large-scale features. More generally, it

Corresponding author: Pieter van Dokkum

[†] <https://github.com/dokkum/maskfill>

can simplify the analysis, particularly when doing object detection and characterization in large datasets.

Methods for filling in masked data range from the extremely simple (replacing all masked pixels by zeros) to the highly complex (machine learning techniques to eliminate gaps in satellite images; Lomelí-Huerta et al. 2022). Most methods use some form of interpolation, either in the form of low order 2D functions that are fit to the surrounding pixels (Sakurai & Shin 2001; Popowicz et al. 2013), or by applying a median filter with a size that exceeds that of the masked features (Kokaram et al. 1995; van Dokkum 2001; Huang et al. 2002). An alternative approach, particularly suited to large scale defects, is to predict missing data by analyzing the Fourier transform of the image (Cooray et al. 2020).

In this paper a new mask-filling method is presented that can be described as “interpolation by extrapolation”: rather than interpolating over a masked region, its edge pixels are extrapolated inward. Although very different in execution, it is similar in spirit to the Fourier methods of Cooray et al. (2020). In its iterative implementation it is akin to classic flood fill algorithms (Newman & Sproull 1979), as well as the cosmic ray identification code `l.a.cosmic` (van Dokkum 2001). The concept is introduced in §2 and its implementation in the `maskfill` Python script is described in §3. Some examples of its operation are presented in §4. A short conclusion is given in §5.

2. METHODOLOGY

2.1. Concept

The central idea is that masked pixels that are adjacent to unmasked pixels should be treated in a different way than masked pixels that are far from any unmasked pixels. In the former case, the true values of the masked pixels can reasonably be expected to be similar to those of their immediate neighbors, whereas in the latter case there is much less information and a greater degree of smoothing is appropriate. For a given pixel at location (x, y) within a masked region, at a distance d from the nearest edge, this concept can be expressed as

$$F_{x,y} = \frac{1}{2d+1} \sum_{n=-d}^d F_{x+d,y+n}, \quad (1)$$

if the nearest edge is in the $+x$ direction and the pixel is not near a corner. A graphic illustration of the concept is shown in Fig. 1.

The number of edge pixels that contribute to the value of a masked pixel is $(2d+1)$. Pixels near the center are averages of many edge pixels, whereas pixels close to the edge are determined by their immediate neigh-

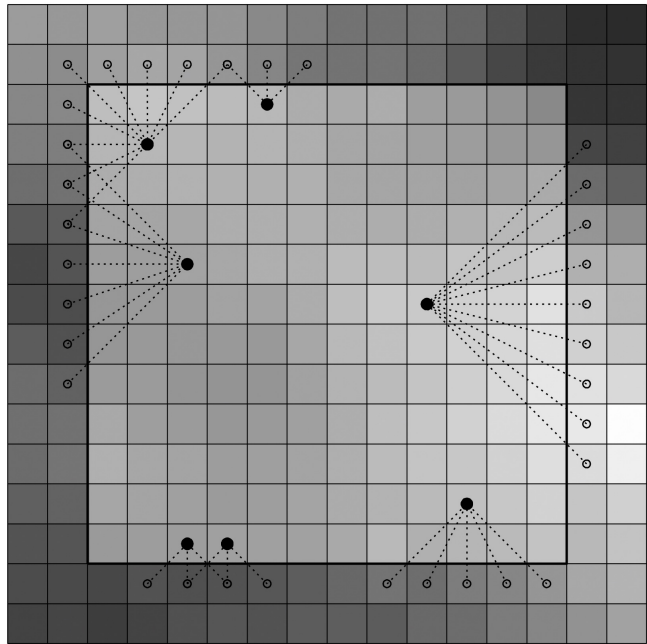


Figure 1. Illustration of the concept. A small (16×16) section of an actual image is shown. The central 12×12 pixels are shown behind a hypothetical semi-transparent mask. Typically all masked pixels are replaced by the same value, or by a low order 2D surface. However, it is clear that there are strong correlations between pixels just outside and just inside the mask. These correlations are maintained if pixels near the edge are filled by the mean or median of only the immediately-adjacent edge pixels. Pixels that are closer to the center are filled by the mean of a larger number of edge pixels, with the number of contributing pixels increasing with the distance to the nearest edge.

bors only. This implies a spatially-dependent smoothing, maintaining high resolution information near the edge and smoothing by \sim half the size of the masked region near the center.

2.2. Iterative Extrapolation of Edges

While possible, it is not straightforward to turn Eq. 1 directly into a practical and efficient application. It would be necessary to find all connected masked pixels and their edges, a task that is complicated by the fact that, in practice, masked regions overlap. As an example, bad columns typically intersect many cosmic rays, producing complex shapes.

Fortunately we can simplify the problem, by making use of the hierarchy that is inherent in Eq. 1. Each pixel that is adjacent to an edge is the average of its three immediate neighbors. As can be deduced from the dotted lines in Fig. 1, *this same rule applies to pixels that are far away from an edge* – the only difference is that the values of the three adjacent pixels are not known a pri-

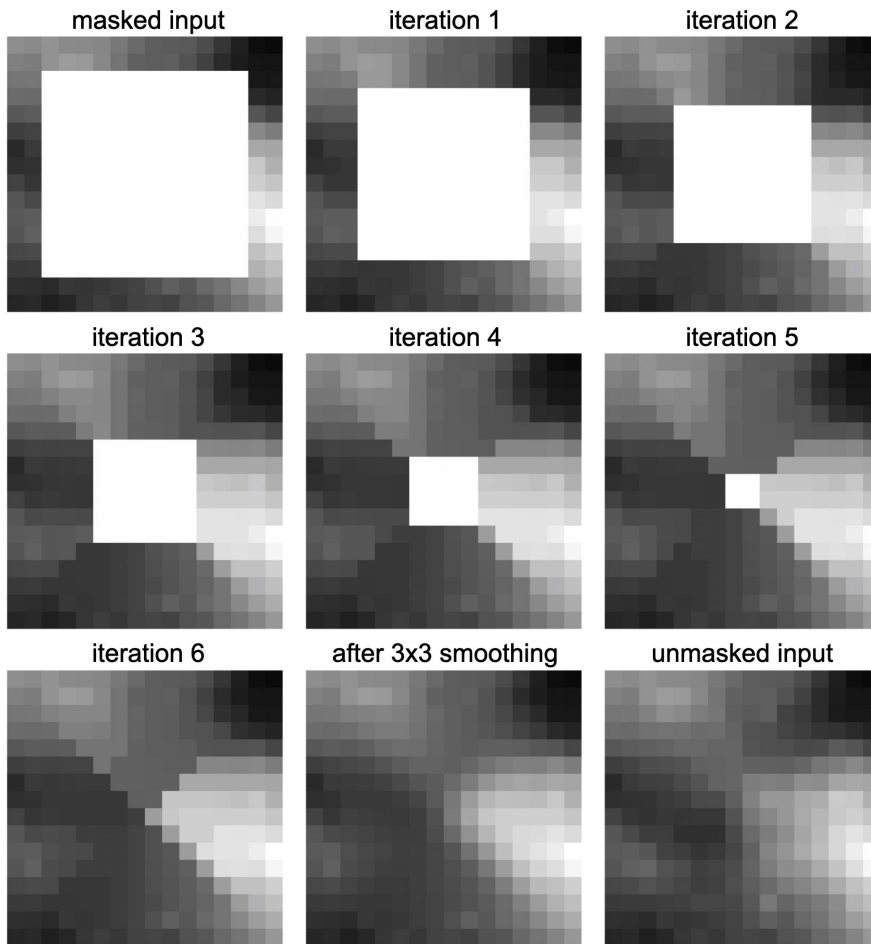


Figure 2. Demonstration of the iterative extrapolation of edge pixels. The masked input image is shown at upper left. In each iteration, pixels inside the mask are replaced by the median of their closest neighbors, by applying a 3×3 filter. The final step is to apply a 3×3 boxcar filter to the now filled-in masked region. In this case, the filled-in region is quite similar to the actual data, shown in the lower right panel.

ori. The solution, then, is to iteratively extrapolate the edges inward, so that each successive layer can be determined from the previous one, using the same operation.

Successive steps in this process are shown in Fig. 2, created with the default version of `maskfill` (described below). In each iteration, a 3×3 median filter is applied to the image (a mean filter produces similar results), until all masked pixels are filled in. The final step in the process is the application of a 3×3 boxcar filter to all pixels within the masked region, to smooth out sharp ridges. These ridges are evident after the sixth iteration, and an artifact of the application of Eq. 1 to a square region. The extrapolations of the four sides are largely independent until they meet in the middle, producing an X-pattern that is characteristic of the method.

The reconstructed image is an excellent match to the truth, shown in the bottom right panel of Fig. 2. This is not always the case (see §5), but it is not unusual: the match is generally good when the mask interrupts a

continuous feature, such as the emission going from top left to bottom right in this example.

3. IMPLEMENTATION

The method is implemented in the Python script `maskfill.py`, distributed via `github` (<https://github.com/dokkum/maskfill>). The script is in essence a repeated application of a (customized) median filter. The code can be run from the command line, via

```
python maskfill.py in.fits mask.fits out.fits
```

The mask consists of 0s and 1s, with 1 indicating that a pixel is masked. The mask image has to have the same dimensions as the input image.

Optional parameters include the nature of the filter (mean or median, with median the default), the size of the filter (default 3), a flag to omit the final smoothing step if desired, and a flag to write out a fits image after each iteration. A 3×3 filter and median filtering

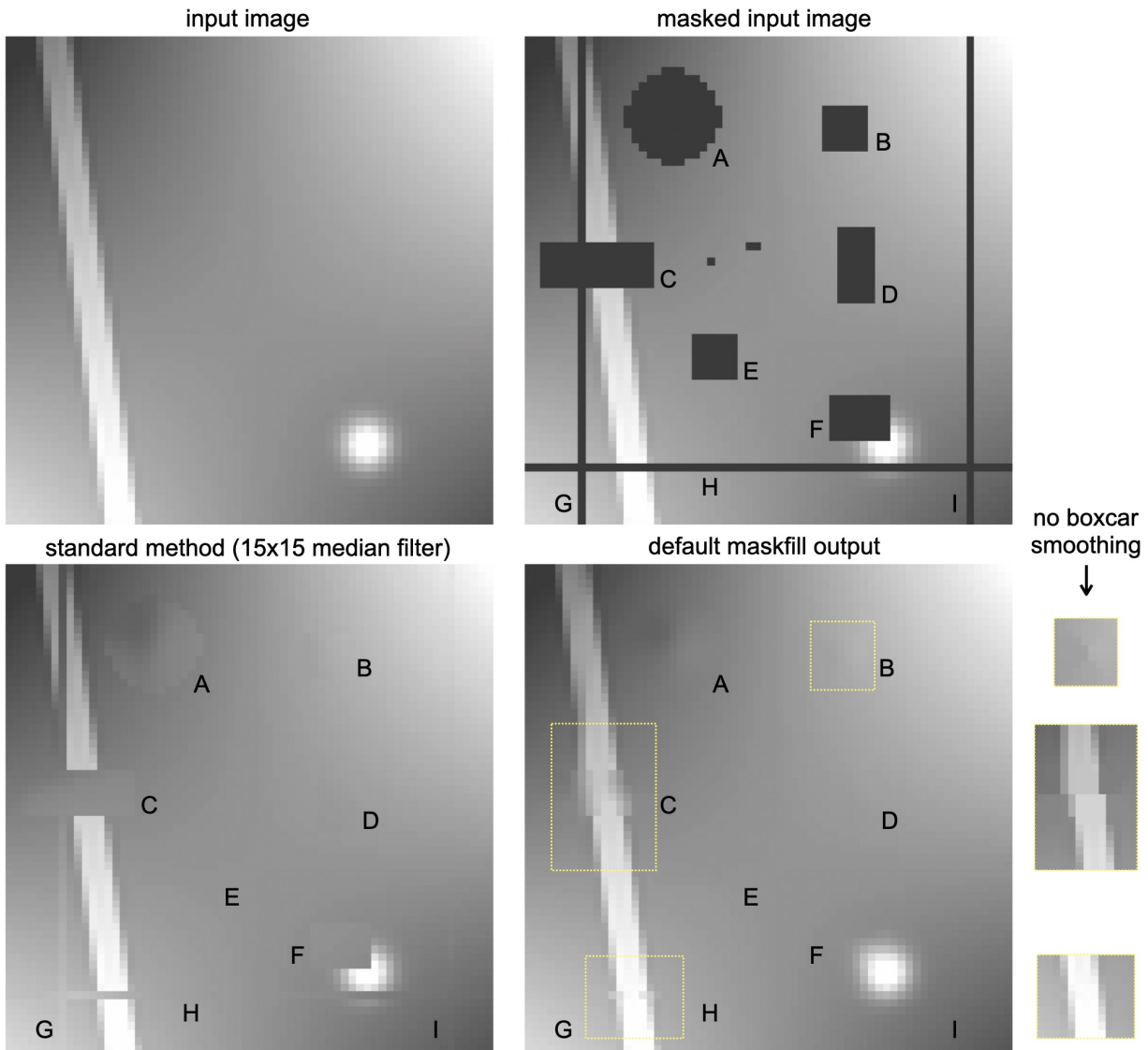


Figure 3. Application to a synthetic image with a variety of structures and masks. The input image and the masked input image are shown at the top. A standard method for filling in masked regions, using a 15×15 pixel median filter applied to unmasked pixels, is shown in lower left. The lower right panel shows the `maskfill` output. The masked row and columns (G, H, I) are nearly identical to the input image, and both the star (F) and the linear feature (C) are reconstructed reasonably well. Insets at right show the effects of setting the `--nosmooth` flag in `maskfill`.

will in almost all cases produce the best results. The main reason to consider deviating from these defaults is speed: the number of iterations is reduced when the size of the filter is increased, and means are computed somewhat faster than medians. Whether to apply the final smoothing is a judgement call, depending on the nature of the image. If there are many sharp features it can be best to omit the smoothing. In most applications any differences will be hardly noticeable.

4. EXAMPLES

4.1. Synthetic Image

The method is first applied to an artificial image of 64×64 pixels, with a smoothly varying background, a linear feature, and a star. Regions of varying shapes and sizes are masked, including a column, a row, and several rectangles (see Fig. 3). Results from a standard method to fill in the mask are shown in the bottom left panel of Fig. 3. Here a 15×15 pixel median filter was applied to the image, excluding all masked pixels. The size of the filter just exceeds the dimensions of the largest masked region. As expected, all masked regions, including those that intersect the linear feature (C) and the star (F), are filled with the local background. This fill method works

well for regions that are far away from objects: B, D, E, and portions of the masked row (H) and columns (G, I).

The output from `maskfill` is shown in the lower right panel. The code performs equally well as the simple 15×15 median filter in empty regions, and much better where the masks intersect objects. The masked portions of the linear feature (C) and the star (F) are reconstructed fairly well. The reconstructions of the masked row and columns are nearly perfect; for features with a width of 1 or 2 pixels, such as bad pixels, hot pixels, bad columns, and many cosmic rays, the code reduces to a straightforward (and optimal) interpolation of the locally-adjacent pixels.

The default settings of `maskfill` include a 3×3 boxcar smoothing at the end. The insets at right show the effects of turning this smoothing off (with the `--nosmooth` flag). The reconstruction of the sharp linear feature is improved, at the cost of having a faint X-pattern in B.

4.2. Cosmic Ray Replacement

While `maskfill` cannot be used to *detect* cosmic rays, it is well-suited to replacing them with plausible values after they are found. A test image was created by adding actual cosmic rays (identified in an HST WFPC2 image) to a deep HST UVIS image (from program GO-17301). Three example galaxies are shown in Fig. 4. The performance of `maskfill` is compared to that of `l.a.cosmic` (van Dokkum 2001). After identifying cosmic rays, `l.a.cosmic` produces a cleaned image by replacing masked pixels with the median of neighboring pixels, using a fixed 5×5 filter. This size is adequate for cosmic rays, as they are always narrow in at least one dimension.

The performance of `maskfill` is indistinguishable from that of the fill step of `l.a.cosmic` in the vast majority of cases, with both methods producing excellent results. In the rare cases where there is a difference, `maskfill` performs better. An example is shown in the bottom panels of Fig. 4: a cosmic ray covers the center of a compact galaxy, and the 5×5 filter of `l.a.cosmic` is too large to reconstruct the affected pixels. For optimal results, `maskfill` can simply be run after `l.a.cosmic`, using the original image and the mask that `l.a.cosmic` produces as inputs.

4.3. Sections of M51

For a more challenging test, the iconic IRAF 512×512 pixel image of M51 was degraded by adding 3000 wide and long cosmic ray-like objects. A few bright stars in the image were also masked. In Fig. 5 the `maskfill` reconstructions of several regions are compared to the unmasked input. The filled images are very similar to

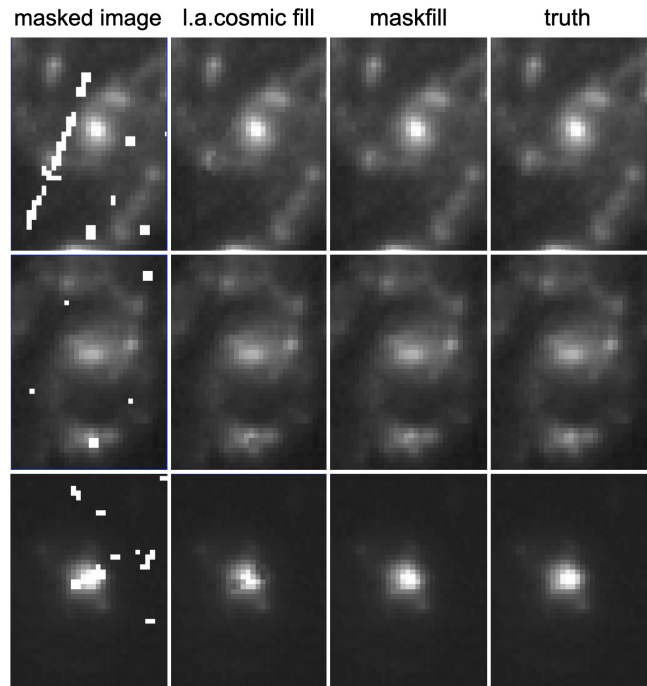


Figure 4. Replacement of cosmic rays, in $1''.2 \times 1''.7$ sections of a deep HST image. The cosmic rays were obtained from an independent image and added to the drizzled data. The `maskfill` code performs slightly better than the fill routine in `l.a.cosmic` (van Dokkum 2001), although differences are small.

the original images, even in cases where several masks intersect. The bottom row of Fig. 5 shows a masked star. The filled-in mask is a plausible continuation of the surrounding emission.

5. CONCLUSIONS

This paper describes `maskfill`, a new method for filling in masked emission in astronomical images. The method is encapsulated in Eq. 1, and implemented as an iterative inward extrapolation of the edges of masked regions. It is available as a Python script, through `github`. Although `maskfill.py` has several optional parameters, no tuning should be necessary: the code works on masks of arbitrary shapes and sizes, always beginning with the pixels that are closest to the edge.

Several caveats and limitations should be mentioned. Even though the algorithm is well-defined it is difficult to assign an uncertainty to the filled-in values. The formal per-pixel noise decreases with d , the distance to the edge of the mask, according to $\sigma_{\text{mask}} = \sigma_{\text{org}} (2d + 1)^{-0.5}$, with σ_{org} the per-pixel noise outside of the mask. However, the reliability of the reconstruction depends on the likelihood of encountering features that do not extend beyond the mask boundaries. The bottom row of Fig. 5

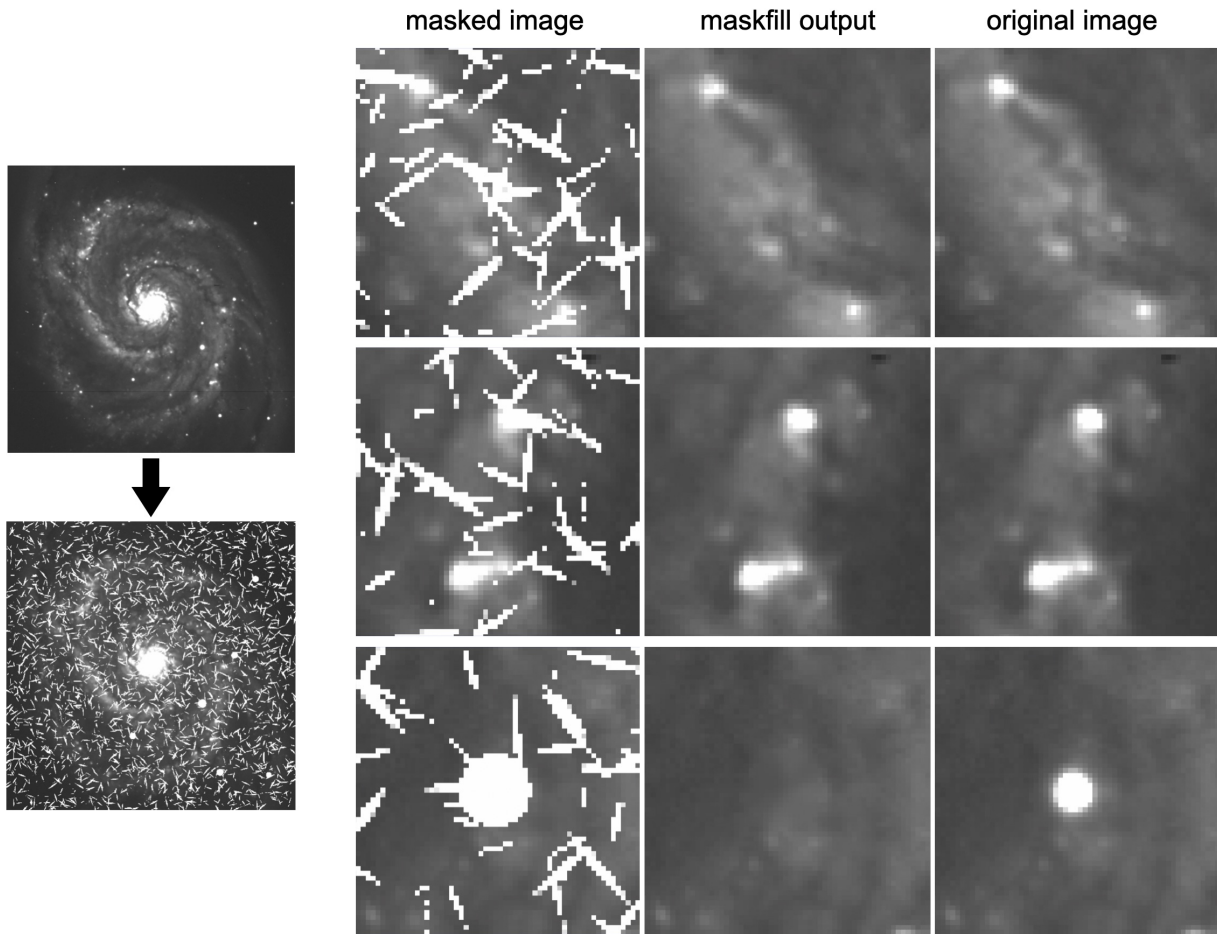


Figure 5. Demonstration on the IRAF M51 image, with a mask containing 3000 thick cosmic ray-like objects. The `maskfill` reconstructions, with default parameters, are shown in the middle column, with the original images at right. The bottom row shows a masked star.

is a good example of this: if the circular mask had been created to cover a defect, the reconstruction would have entirely missed the star at that location. Fortunately, most detector defects and cosmic rays are on scales of a few pixels, where the code is reliable and its behavior is predictable. Larger masks are often created to mask objects, and in those cases the whole point is *not* to match reality but to replace the masked region with something that fits in with its surroundings.

Another limitation is the characteristic cross pattern that arises on smoothly varying backgrounds, particularly within square regions. This is inherent in the method: the extrapolation begins on the four edges and then works its way inward. When the filled-in pixels finally meet in the center, they each represent a different edge, with almost no knowledge of the other three edges. The boxcar smoothing step at the end reduces

this artifact, at a cost of a slight loss of resolution. This trade-off is illustrated in Fig. 3.

Lastly, version 1.0 of the code is relatively slow, needing about 200 s per iteration on a 2019 Macbook Pro when analyzing a 2048×2048 image. In each iteration a loop through the entire image is done, and a median of surrounding pixels is calculated for each position. The median filter in `scipy.ndimage` would be significantly faster, but it does not allow the necessary rejection and condition testing.

The `maskfill` code makes use of `NumPy`, a package for scientific computing with Python (Walt et al. 2011); and `Astropy`, a community-developed core Python package for Astronomy (Price-Whelan & Astropy Collaboration 2018). Several example images were created with `IRAF`, the Image Reduction and Analysis Facility (Tody 1986, 1993).

REFERENCES

- Cooray, S., Takeuchi, T. T., Yoda, M., & Sorai, K. 2020, *PASJ*, 72, 61
- Danieli, S. & van Dokkum, P. 2019, *ApJ*, 875, 155
- Fruchter, A. S. & Hook, R. N. 2002, *PASP*, 114, 144
- Garner, R., Mihos, J. C., Harding, P., Watkins, A. E., & McGaugh, S. S. 2022, *ApJ*, 941, 182
- Greco, J. P., Greene, J. E., Strauss, M. A., Macarthur, L. A., Flowers, X., Goulding, A. D., Huang, S., Kim, J. H., Komiyama, Y., Leauthaud, A., Leisman, L., Lupton, R. H., Sifón, C., & Wang, S.-Y. 2018, *ApJ*, 857, 104
- Huang, H.-C., Cressie, N., & Gabrosek, J. 2002, *Journal of Computational and Graphical Statistics*, 11, 63
- James, P. A., Shane, N. S., Beckman, J. E., Cardwell, A., Collins, C. A., Etherton, J., de Jong, R. S., Fathi, K., Knapen, J. H., Peletier, R. F., Percival, S. M., Pollacco, D. L., Seigar, M. S., Stedman, S., & Steele, I. A. 2004, *A&A*, 414, 23
- Kelson, D. D. 2003, *PASP*, 115, 688
- Kessler, R., Marriner, J., Childress, M., Covarrubias, R., D'Andrea, C. B., Finley, D. A., Fischer, J., & DES Collaboration. 2015, *AJ*, 150, 172
- Kokaram, A., Morris, R., Fitzgerald, W., & Rayner, P. 1995, *IEEE Transactions on Image Processing*, 4, 1509
- Leach, R. W. & Gursky, H. 1979, *PASP*, 91, 855
- Liu, Q., Abraham, R., Martin, P. G., Bowman, W. P., van Dokkum, P., Janssens, S. R., Chen, S., Keim, M. A., Lokhorst, D., Pasha, I., Shen, Z., & Zhang, J. 2023, *ApJ*, 953, 7
- Lokhorst, D., Abraham, R., Pasha, I., van Dokkum, P., Chen, S., Miller, T., Danieli, S., Greco, J., Zhang, J., Merritt, A., & Conroy, C. 2022, *ApJ*, 927, 136
- Lomelí-Huerta, J. R., Rivera-Caicedo, J. P., De-la-Torre, M., Acevedo-Juárez, B., Cepeda-Morales, J., & Avila-George, H. 2022, *PeerJ Comput Sci.*, 8, e979
- Marois, C., Lafrenière, D., Doyon, R., Macintosh, B., & Nadeau, D. 2006, *ApJ*, 641, 556
- Montes, M. & Trujillo, I. 2018, *MNRAS*, 474, 917
- Neill, D., Matuszewski, M., Martin, C., Brodheim, M., & Rizzi, L. 2023, *KCWI.DRP: Keck Cosmic Web Imager Data Reduction Pipeline in Python*, *Astrophysics Source Code Library*, record ascl:2301.019
- Newman, W. M. & Sproull, R. F. 1979, *Principles of Interactive Computer Graphics* (2nd edition) (New York: McGraw-Hill)
- Peng, C. Y., Ho, L. C., Impey, C. D., & Rix, H.-W. 2002, *AJ*, 124, 266
- Popowicz, A., Kurek, A. R., & Filus, Z. 2013, *PASP*, 125, 1119
- Price-Whelan, A. M. & Astropy Collaboration. 2018, *AJ*, 156, 123
- Sakurai, T. & Shin, J. 2001, *PASJ*, 53, 361
- Tody, D. 1986, in *Proc. SPIE*, Vol. 627, *Instrumentation in astronomy VI*, ed. D. L. Crawford, 733
- Tody, D. 1993, in *Astronomical Society of the Pacific Conference Series*, Vol. 52, *Astronomical Data Analysis Software and Systems II*, ed. R. J. Hanisch, R. J. V. Brissenden, & J. Barnes, 173
- van Dokkum, P., Lokhorst, D., Danieli, S., Li, J., Merritt, A., Abraham, R., Gilhuly, C., Greco, J. P., & Liu, Q. 2020, *PASP*, 132, 074503
- van Dokkum, P. G. 2001, *PASP*, 113, 1420
- Walt, S. v. d., Colbert, S. C., & Varoquaux, G. 2011, *Computing in Science and Engg.*, 13, 22